6.2 Conductance-Based Models

conductance-based model

The electrical properties of neurons arise from membrane conductances with a wide variety of properties. The basic formalism developed by Hodgkin and Huxley to describe the Na^+ and K^+ conductances responsible for generating action potentials (discussed in chapter 5) is also used to represent most of the additional conductances encountered in neuron modeling. Models that treat these aspects of ionic conductances, known as conductance-based models, can reproduce the rich and complex dynamics of real neurons quite accurately. In this chapter, we discuss both single- and multi-compartment conductance-based models, beginning with the single-compartment case.

To review from chapter 5, the membrane potential of a single-compartment neuron model, V, is determined by integrating the equation

$$c_{\rm m}\frac{dV}{dt} = -i_{\rm m} + \frac{I_{\rm e}}{A}\,. \tag{6.1}$$

with $I_{\rm e}$ the electrode current, A the membrane surface area of the cell, and $i_{\rm m}$ the membrane current. In the following subsections, we present expressions for the membrane current in terms of the reversal potentials, maximal conductance parameters, and gating variables of the different conductances of the models being considered. The gating variables and V comprise the dynamic variables of the model. All the gating variables are determined by equations of the form

$$\tau_z(V)\frac{dz}{dt} = z_\infty(V) - z \tag{6.2}$$

where we have used the letter z to denote a generic gating variable. The functions $\tau_z(V)$ and $z_\infty(V)$ are determined from experimental data. For some conductances, these are written in terms of the open and closing rates $\alpha_z(V)$ and $\beta_z(V)$ (see chapter 5) as

$$\tau_z(V) = \frac{1}{\alpha_z(V)+\beta_z(V)} \quad \text{and} \quad z_\infty(V) = \frac{\alpha_z(V)}{\alpha_z(V)+\beta_z(V)}\,. \tag{6.3}$$

We have written $\tau_z(V)$ and $z_\infty(V)$ as functions of the membrane potential, but for Ca^{2+}-dependent currents they also depend on the internal Ca^{2+} concentration. We call the $\alpha_z(V)$, $\beta_z(V)$, $\tau_z(V)$, and $z_\infty(V)$ collectively gating functions. A method for numerically integrating equations 6.1 and 6.2 is described in the appendices of chapter 5.

In the following subsections, some basic features of conductance-based models are presented in a sequence of examples of increasing complexity. We do this to illustrate the effects of various conductances and combinations of conductances on neuronal activity. Different cells (and even the same cell held at different resting potentials) can have quite different response properties due to their particular combinations of conductances.

Research on conductance-based models focuses on understanding how neuronal response dynamics arises from the properties of membrane and synaptic conductances, and how the characteristics of different neurons interact when they are coupled to each other in networks.

The Connor-Stevens Model

The Hodgkin-Huxley model of action potential generation, discussed in chapter 5, was developed on the basis of data from the giant axon of the squid, and we present a multi-compartment simulation of action potential propagation using this model in a later section. The Connor-Stevens model (Connor and Stevens, 1971; Connor et al. 1977) provides an alternative description of action potential generation. Like the Hodgkin-Huxley model, it contains fast Na^+, delayed-rectifier K^+, and leakage conductances. The fast $Na^+$and delayed-rectifier K^+ conductances have somewhat different properties from those of the Hodgkin-Huxley model, in particular faster kinetics, so the action potentials are briefer. In addition, the Connor-Stevens model contains an extra K^+ conductance, called the A-current, that is transient. K^+ conductances come in wide variety of different forms, and the Connor-Stevens model involves two of them.

A-type potassium current

The membrane current in the Connor-Stevens model is

$$i_{\rm m} = \overline{g}_L(V - E_{\rm L}) + \overline{g}_{\rm Na} m^3 h(V - E_{\rm Na}) + \overline{g}_K n^4 (V - E_{\rm K}) + \overline{g}_{\rm A} a^3 b(V - E_{\rm A}) \tag{6.4}$$

where $\overline{g}_{\rm L} = 0.003$ mS / mm^2 and $E_{\rm L}$ = -17 mV are the maximal conductance and reversal potential for the leak conductance, and $\overline{g}_{\rm Na} = 1.2$ mS / mm^2, $\overline{g}_{\rm K} = 0.2$ mS / mm^2, $\overline{g}_{\rm A} = 0.477$ mS / mm^2, $E_{\rm Na}$ = 55 mV, $E_{\rm K}$ = -72 mV, and $E_{\rm A}$ = -75 mV (although the A-current is carried by K^+, the model does not require $E_{\rm A} = E_{\rm K}$) and are similar parameters for the active conductances. The gating variables, *m*, *h*, *n*, *a*, and *b*, are determined by equations of the form 6.2 with the gating functions given in appendix A.

The fast Na^+ and delayed-rectifier K^+ conductances generate action potentials in the Connor-Stevens model just as they do in the Hodgkin-Huxley model (see chapter 5). What is the role of the additional A-current? Figure 6.1 illustrates action potential generation in the Connor-Stevens model. In the absence of an injected electrode current or synaptic input, the membrane potential of the model remains constant at a resting value of -68 mV. For a constant electrode current greater than a threshold value, the model neuron generates action potentials. Figure 6.1A shows how the firing rate of the model depends on the magnitude of the electrode current relative to the threshold value. The firing rate rises continuously from zero and then increases roughly linearly for currents over the range shown. Figure 6.1B shows an example of action potential generation for one particular value of the electrode current.

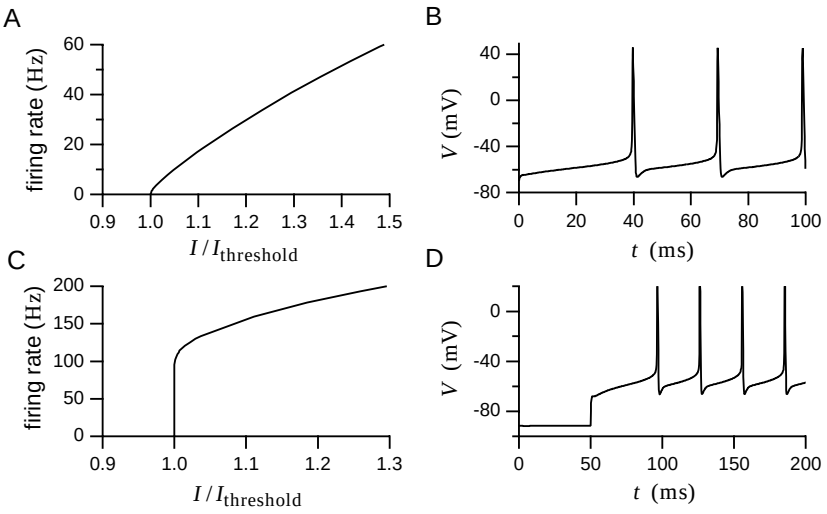

Figure 6.1: Firing of action potentials in the Connor-Stevens model. A) Firing rate as a function of electrode current. The firing rate rises continuously from zero as the current increases beyond the threshold value. B) An example of action potentials generated by constant current injection. C) Firing rate as a function of electrode current when the A-current is turned off. The firing rate now rises discontinuously from zero as the current increases beyond the threshold value. D) Delayed firing due to hyperpolarization. The neuron was held hyperpolarized for a prolonged period by injection of negative current. At $t = 50$ ms, the negative electrode current was switched to a positive value. The A-current delays the occurrence of the first action potential.

Figure 6.1C shows the firing rate as a function of electrode current for the Connor-Stevens model with the maximal conductance of the A-current set to zero. The leakage conductance and reversal potential have been adjusted to keep the resting potential and membrane resistance the same as in the original model. The firing rate is clearly much higher with the A-current turned off. This is because the deinactivation rate of the A-current limits the rise time of the membrane potential between action potentials. In addition, the transition from no firing for currents less than the threshold value to firing with suprathreshold currents is different when the A-current is eliminated. Without the A-current, the firing rate jumps discontinuously to a nonzero value rather than rising continuously. Neurons with firing rates that rise continuously from zero as a function of electrode current are called type I, and those with discontinuous jumps in their firing rates at threshold are called type II. An A-current is not the only mechanism that can produce a type I response but, as figures 6.1A and 6.1C show, it plays this role in the Connor-Stevens model. The Hodgkin-Huxley model produces a type II response.

type I, type II

Another effect of the A-current is illustrated in figure 6.1D. Here the model neuron was held hyperpolarized by negative current injection for an ex-

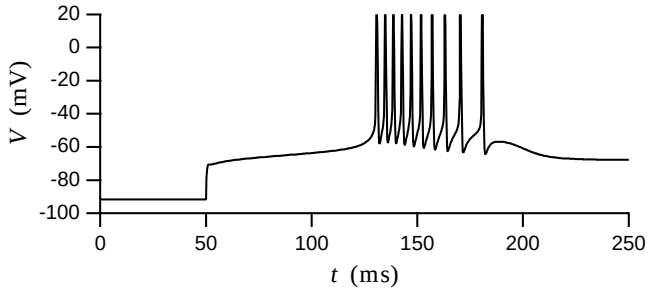

Figure 6.2: A burst of action potentials due to rebound from hyperpolarization. The model neuron was held hyperpolarized for an extended period (until the conductances came to equilibrium) by injection of constant negative electrode current. At $t = 50$ ms, the electrode current was set to zero, and a burst of Na^+ spikes was generated due to an underlying Ca^{2+} spike. The delay in the firing is caused by the presence of the A-current in the model.

tended period of time, and then the current was switched to a positive value. While the neuron was hyperpolarized, the A-current deinactivated, that is, the variable *b* increased toward one. When the electrode current switched sign and the neuron depolarized, the A-current first activated and then inactivated. This delayed the first spike following the change in the electrode current.

Postinhibitory Rebound and Bursting

transient Ca^{2+} conductance

The range of responses exhibited by the Connor-Stevens model neuron can be extended by including a transient Ca^{2+} conductance. The conductance we use was modeled by Huguenard and McCormick (1992) on the basis of data from thalamic relay cells. The membrane current due to the transient Ca^{2+} conductance is expressed as

$$i_{\mathrm{CaT}} = \overline{g}_{\mathrm{CaT}} M^2 H (V - E_{\mathrm{Ca}}) \tag{6.5}$$

with, for the example given here, $\overline{g}_{\mathrm{CaT}} = 13\ \mu\mathrm{S/mm}^2$ and $E_{\mathrm{Ca}} = 120$ mV. The gating variables for the transient Ca^{2+} conductance are determined from the gating functions in appendix A.

L, T, N and P type Ca^{2+} channels

Several different Ca^{2+} conductances are commonly expressed in neuronal membranes. These are categorized as L, T, N, and P types. L-type Ca^{2+} currents are persistent as far as their voltage dependence is concerned, and they activate at a relatively high threshold. They inactivate due to a Ca^{2+}-dependent rather than voltage-dependent process. T-type Ca^{2+} currents have lower activation thresholds and are transient. N- and P-type Ca^{2+} conductances have intermediate thresholds and are respectively transient and persistent. They may be responsible for the Ca^{2+} entry that causes the release of transmitter at presynaptic terminals. Entry of Ca^{2+} into a neuron

6.5 Chapter Summary

We continued the discussion of neuron modeling that began in chapter 5 by considering models with more complete sets of conductances and techniques for incorporating neuronal morphology. We introduced A-type K^+, transient Ca^{2+}, and Ca^{2+}-dependent K^+ conductances and noted their effect on neuronal activity. The cable equation and its linearized version were introduced to examine the effects of morphology on membrane potentials. Finally, multi-compartment models were presented and used to discuss propagation of action potentials along unmyelinated and myelinated axons.

6.6 Appendices

A) Gating Functions for Conductance-Based Models

Connor-Stevens Model

The rate functions used for the gating variables n, m, and h of the Connor-Stevens model, in units of $1/\text{ms}$ with V in units of mV, are

$$\begin{aligned} \alpha_m &= \frac{0.38(V+29.7)}{1-\exp[-0.1(V+29.7)]} \quad & \beta_m &= 15.2\exp[-0.0556(V+54.7)] \\ \alpha_h &= 0.266\exp[-0.05(V+48)] & \beta_h &= 3.8/(1+\exp[-0.1(V+18)]) \\ \alpha_n &= \frac{0.02(V+45.7)}{1-\exp[-.1(V+45.7)]} & \beta_n &= 0.25\exp[-0.0125(V+55.7)]\,. \end{aligned} \tag{6.33}$$

The A-current is described directly in terms of the asymptotic values and τ functions for its gating variables (with τ_a and τ_b in units of ms and V in units of mV),

$$a_\infty = \left[\frac{0.0761\exp[0.0314(V+94.22)]}{1+\exp[0.0346(V+1.17)]}\right]^{1/3} \tag{6.34}$$

$$\tau_a = 0.3632 + 1.158/(1+\exp[0.0497(V+55.96)]) \tag{6.35}$$

$$b_\infty = \left[\frac{1}{1+\exp[0.0688(V+53.3)]}\right]^4 \tag{6.36}$$

and

$$\tau_b = 1.24 + 2.678/(1+\exp[0.0624(V+50)])\,. \tag{6.37}$$